Computers and Concrete, *Vol. 17, No. 5 (2016) 567-578*
DOI: http://dx.doi.org/10.12989/cac.2016.17.5.567

Buckling analysis of embedded concrete columns armed with carbon nanotubes

Ali Jafarian Arani and Reza Kolahchi*

Department of Civil Engineering, Khomein Branch, Islamic Azad University, Khomein, Iran

(Received January 9, 2016, Revised March 17, 2016, Accepted March 21, 2016)

Abstract. As concrete is most usable material in construction industry it's been required to improve its quality. Nowadays, nanotechnology offers the possibility of great advances in construction. For the first time, the nonlinear buckling of straight concrete columns armed with single-walled carbon nanotubes (SWCNTs) resting on foundation is investigated in the present study. The column is modelled with Euler-Bernoulli and Timoshenko beam theories. The characteristics of the equivalent composite being determined using mixture rule. The foundation around the column is simulated with spring and shear layer. Employing nonlinear strains-displacements, energy methods and Hamilton's principal, the governing equations are derived. Differential quadrature method (DQM) is used in order to obtain the buckling load of structure. The influences of volume percent of SWCNTs, geometrical parameters, elastic foundation and boundary conditions on the buckling of column are investigated. Numerical results indicate that reinforcing the concrete column with SWCNTs, the structure becomes stiffer and the buckling load increases with respect to concrete column armed with steel.

Keywords: concrete column; SWCNTs; DQM; buckling, foundation

1. Introduction

Typical concretes consist of ordinary Portland cement (OPC), fillers such as sand, coarse aggregates, admixtures and water. This combination of materials allows concrete to be produced in a fluid form that can be pumped and moulded. The complex chemistry and physical structure of cement hydrates in concrete however mean that issues of fundamental science still need to be resolved. Research at the nanoscale has the potential to contribute to these debates and questions. Analysis at the nanoscale may provide further insight into the nature of hydrated cement phases and their interaction with admixtures, nanofillers and nanofibers. These interactions offer the possibility of modifying cement reactions, creating new surface chemistries (referred to as nanoscience), developing new products for the concrete industry (referred to as nanotechnology), and allowing a more controlled and ecologically friendly manufacturing route to cement and concrete.

Buckling of concrete column has been investigated by many researchers. The first who studied

*Corresponding author, Professor., E-mail: r.kolahchi@gmail.com

http://www.techno-press.org/?journal=cac&subpage=8 ISSN: 1598-8198 (Print), 1598-818X (Online)

theoretically the buckling stability of elasto-plastic columns appeared to be Engesser (1889). He proved that the material non-linearity can largely reduce the buckling load. Further, he raised the important question how the column unloads, and suggested that the buckling load of an inelastic column must be obtained from Euler's formulae. This question was only correctly resolved later on by Shanley (1947) who, with the help of the simple theoretical model and various experiments, showed that the buckling of an elastic-plastic column occurs at the so-called tangent critical load. Mau (1990) and Mau and El-Mabsout (1989) developed a beam-column element for the finite element inelastic buckling analysis to determine the column load-carrying capacity. Pantazopoulou (1998) compiled data from the literature of over 300 column tests and developed requirements for reinforcement stability that recognize the interaction between displacement ductility demand in critical section, tie effectiveness, limiting concrete strain, bar size and tie spacing. Dhakal and Maekawa (2002a) used fiber finite element analyses to present an average compressive stress-strain relation for reinforcing bars as a function of slenderness ratio and yield strength. Later, Bae *et al*. (2005) conducted an experimental program study on bar buckling and examined the effects of three important bar parameters, the L/D ratio (length over bar diameter), e/D (initial imperfection over bar diameter) ratio and the ratio of ultimate strength to yield strength. Dhakal and Maekawa (2002b) derived a method to predict the buckling length of longitudinal reinforcing bars using an energy method. The exact analytical solutions for the buckling loads of a reinforced concrete Euler-type column are presented in, e.g. Krauberger *et al*. (2007), where the effect of the material non-linearity on the buckling load is fully assessed. The development of a finite element model for the geometric and material nonlinear analysis of bonded prestressed concrete continuous beams was presented by Lou *et al*. (2015). Bajc *et al*. (2015) derived a new semi-analytical procedure for the determination of buckling of the reinforced concrete column exposed to fire. An experimental investigation on the behaviour of geopolymer composite concrete beams reinforced with conventional steel bars and various types of fibres namely steel, polypropylene and glass in different volume fractions under flexural loading was presented by Vijai *et al*. (2015). Choi *et al*. (2015) conducted shear tests on steel fiber reinforced-prestressed concrete (SFR-PSC) members with test parameters of the concrete compressive strength, the volume fraction of steel fibers, and the level of effective prestress. Nominal moment-axial load interaction diagrams, moment-curvature relationships, and ductility of rectangular hybrid beam-column concrete sections were analysed by El-Helou and Aboutaha (2015) using the modified Hognestad concrete model.

It can be observed from literature that the theoretical researches on buckling of concrete columns armed with SWCNTs are rare. The main goal of the present paper is to present a mathematical model for concrete columns and discuss about the nanotechnology effects. For this ends, the concrete column is modelled with Euler-Bernoulli and Timoshenko beam models. The foundation is simulated with spring and shear constants. Applying energy method and Hamilton’s principal, the governing equations are derived. DQM is used for obtaining the buckling load of structure. The effects of different parameters such as volume percent of SWCNTs, geometrical parameters, elastic foundation and boundary conditions on the buckling of concrete columns are discussed.

2. Mathematical modelling

Fig. 1 shows a SWCNT-reinforced concrete column with length L and thickness h embedded in foundation. The surrounding foundation is described by the Winkler foundation model with spring

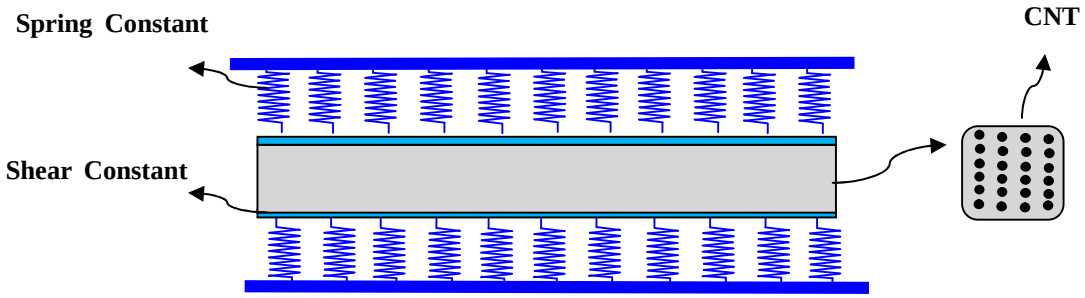

Fig. 1 Geometry of the concrete column resting on foundation

constant K_w and Pasternak foundation model with shear constant G_p.

2.1 Displacement fields

The concrete column is modelled with beam. The displacements of an arbitrary point in the beam are (Brush and Almroth 1975)

$$\begin{aligned} u_1(x,z) &= U(x) - z\frac{\partial W(x)}{\partial x} + f(z)\left(\psi(x) + z\frac{\partial W(x)}{\partial x}\right), \\ u_2(x,z) &= 0, \\ u_3(x,z) &= W(x), \end{aligned} \tag{1}$$

where $U(x, t)$ and $W(x, t)$ are displacement components in the mid-plane, ψ is the rotation of beam cross-section. Noted that $f(z)=0$ and $f(z)=1$ are related to Euler-Bernoulli and Timoshenko beam models. The von Karman type nonlinear strain–displacement relations are given by

$$\varepsilon_{xx} = \frac{\partial U}{\partial x} + \frac{1}{2}\left(\frac{\partial W}{\partial x}\right)^2 - z\frac{\partial^2 W(x)}{\partial x^2} + f(z)\left(\frac{\partial \psi(x)}{\partial x} + z\frac{\partial^2 W(x)}{\partial x^2}\right), \tag{2}$$

$$\gamma_{xz} = f(z)\left(\frac{\partial W}{\partial x} + \psi\right). \tag{3}$$

2.2 Stress-strain relations

For a beam structure, the constitutive relations can be approximated to one-dimensional form as

$$\sigma_{xx} = C_{11}\varepsilon_x, \tag{4}$$

$$\sigma_{xz} = C_{55} f(z)\left[\frac{\partial W}{\partial x} + \psi\right], \tag{5}$$

where C_{11} and C_{55} are elastic constants.

2.3 Energy method

The strain energy of the structure can be expressed as

$$U = \frac{1}{2}\int_0^L \int_A (\sigma_{xx}\varepsilon_{xx} + 2f(z)\sigma_{xz}\varepsilon_{xz})\, dAdx. \tag{6}$$

Submitting Eqs. (2) and (3) into (6) gives

$$U = \frac{1}{2}\int_0^l \int_A \left\{ N_x \left[\frac{\partial U}{\partial x} + \frac{1}{2}\left(\frac{\partial W}{\partial x}\right)^2 + f(z)\left(\frac{\partial \psi(x)}{\partial x} + z\frac{\partial^2 W(x)}{\partial x^2} \right) \right] - M_x \frac{\partial^2 W(x)}{\partial x^2} + Q_x f(z)\left[\frac{\partial W}{\partial x} + \psi \right] \right\} dx, \tag{7}$$

where the resultant force (N_x, Q_x) and bending moment M_x, are defined as

$$N_x = \int_A \sigma_{xx}\, dA, \tag{8}$$

$$M_x = \int_A \sigma_{xx} z\, dA, \tag{9}$$

$$Q_x = K_s \int_A \sigma_{xz}\, dA, \tag{10}$$

where K_s is shear correction factor. The work done by the foundation is denoted by (Ghorbanpour Arani *et al*. 2015, Kolahchi *et al*. 2015a)

$$\Omega = \int_0^L \left(\underbrace{-K_w W + G_p \nabla^2 W}_{q} \right) W dx. \tag{11}$$

2.4 Governing equations

The governing equations of structure can be derived from the Hamilton's principle as

$$\int_{t_0}^{t_1} [\delta U - \delta W] = 0. \tag{12}$$

Using above relation, the governing equations may be derived as

• ***Euler-Bernoulli beam model***

$$\delta U : \frac{\partial N_x}{\partial x} = 0, \tag{13}$$

$$\delta W : \frac{\partial^2 M_x}{\partial x^2} - \frac{\partial}{\partial x}\left(N_x^M \frac{\partial W}{\partial x} \right) + q = 0. \tag{14}$$

•***Timoshenko beam model***

$$\frac{\partial N_x}{\partial x} = 0, \tag{15}$$

$$\frac{\partial Q_x}{\partial x} - \frac{\partial}{\partial x}\left(N_x^M \frac{\partial W}{\partial x} \right) + q = 0, \tag{16}$$

$$\frac{\partial M_x}{\partial x} - Q_x = 0, \tag{17}$$

where N_x^M is the axial load applied to the concrete column. Substituting Eqs. (4) and (5) into Eqs. (8)-(10) yields

$$N_x = C_{11} A \frac{\partial U}{\partial x} + \frac{1}{2} C_{11} A \left(\frac{\partial W}{\partial x} \right)^2, \tag{18}$$

$$M_x = C_{11} I \left[-\frac{\partial^2 W}{\partial x^2} + f(z) \left(\frac{\partial \psi}{\partial x} + \frac{\partial^2 W}{\partial x^2} \right) \right], \tag{19}$$

$$Q_x = K_s C_{55} A \left[\frac{\partial W}{\partial x} + \psi \right]. \tag{20}$$

Substituting Eqs. (18)-(20) into the governing equations yields

• ***Euler-Bernoulli beam model***

$$C_{11} \frac{\partial^2 U}{\partial x^2} + C_{11} \frac{\partial^2 W}{\partial x^2} \frac{\partial W}{\partial x} = 0, \tag{21}$$

$$-C_{11} I \frac{\partial^4 W}{\partial x^4} - N_x^M \frac{\partial^2 W}{\partial x^2} - K_w W + G_p \nabla^2 W = 0. \tag{22}$$

• ***Timoshenko beam model***

$$C_{11} \frac{\partial^2 U}{\partial x^2} + C_{11} \frac{\partial^2 W}{\partial x^2} \frac{\partial W}{\partial x} = 0, \tag{23}$$

$$C_{55} A \left[\frac{\partial^2 W}{\partial x^2} + \frac{\partial \psi}{\partial x} \right] - N_x^M \frac{\partial^2 W}{\partial x^2} - K_w W + G_p \nabla^2 W = 0, \tag{24}$$

$$C_{11} I \frac{\partial^2 \psi}{\partial x^2} + K_s C_{55} A \left[\frac{\partial W}{\partial x} + \psi \right] = 0. \tag{25}$$

Introducing the following dimensionless quantities

$$\xi = \frac{x}{L},\ (\overline{W},\overline{U}) = \frac{(W,U)}{h},\ \eta = \frac{h}{L},\psi = \overline{\psi},\ \overline{K}_w = \frac{K_w hL}{C_{11}A},$$
$$\overline{G}_p = \frac{G_p}{C_{11}A},\overline{N}_x^M = \frac{N_x^M}{C_{11}A},\bar{I} = \frac{I}{AL^2},\ C_5 = \frac{C_{55}}{C_{11}}. \tag{26}$$

The governing equations may be written as

• ***Euler-Bernoulli beam model***

$$\frac{\partial^2\overline{U}}{\partial\xi^2} + \eta\frac{\partial^2\overline{W}}{\partial\xi^2}\frac{\partial\overline{W}}{\partial\xi} = 0, \tag{27}$$

$$-\bar{I}\frac{\partial^4\overline{W}}{\partial\xi^4} - \overline{N}_x^M\eta\frac{\partial^2\overline{W}}{\partial\xi^2} - \overline{K}_w\overline{W} + \overline{G}_p\eta\left(\frac{\partial^2\overline{W}}{\partial\xi^2}\right) = 0. \tag{28}$$

• ***Timoshenko beam model***

$$\frac{\partial^2\overline{U}}{\partial\xi^2} + \eta\frac{\partial^2\overline{W}}{\partial\xi^2}\frac{\partial\overline{W}}{\partial\xi} = 0, \tag{29}$$

$$C_5\left[\eta\frac{\partial^2\overline{W}}{\partial\xi^2} + \frac{\partial\overline{\psi}}{\partial\xi}\right] - \overline{N}_x^M\eta\frac{\partial^2\overline{W}}{\partial\xi^2} - \overline{K}_w\overline{W} + \overline{G}_p\frac{\partial^2\overline{W}}{\partial\xi^2} = 0, \tag{30}$$

$$\bar{I}\frac{\partial^2\overline{\psi}}{\partial\xi^2} + K_s C_5\left[\eta\frac{\partial\overline{W}}{\partial\xi} + \overline{\psi}\right] = 0. \tag{31}$$

The associated boundary conditions can be expressed as

• ***Clamped-clamped boundary condition (C-C)***

$$\begin{aligned}\overline{W} = \overline{U} = \overline{\psi} = \frac{\partial\overline{W}}{\partial\xi} = 0, &\qquad @\quad \xi = 0\\ \overline{W} = \overline{U} = \overline{\psi} = \frac{\partial\overline{W}}{\partial\xi} = 0. &\qquad @\quad \xi = 1\end{aligned} \tag{32}$$

• ***Clamped-simply boundary condition (C-S)***

$$\begin{aligned}\overline{W} = \overline{U} = \overline{\psi} = \frac{\partial\overline{W}}{\partial\xi} = 0, &\qquad @\quad \xi = 0\\ \overline{W} = \overline{U} = \frac{\partial\overline{\psi}}{\partial\xi} = \frac{\partial^2\overline{W}}{\partial\xi^2} = 0. &\qquad @\quad \xi = 1\end{aligned} \tag{33}$$

• ***Simply-Simply boundary condition (S-S)***

$$\begin{aligned} \overline{W} = \overline{U} = \frac{\partial \overline{\psi}}{\partial \xi} = \frac{\partial^2 \overline{W}}{\partial \xi^2} = 0, \qquad @ \quad \xi = 0 \\ \overline{W} = \overline{U} = \frac{\partial \overline{\psi}}{\partial \xi} = \frac{\partial^2 \overline{W}}{\partial \xi^2} = 0. \qquad @ \quad \xi = 1 \end{aligned} \tag{34}$$

3. Mixture rule

According to mixture rule, the effective Young and shear moduli of structure can be written as (Kolahchi *et al*. 2015b)

$$E_{11} = \eta_1 c_r E_{r11} + (1 - c_r) E_m, \tag{35}$$

$$\frac{\eta_2}{E_{22}} = \frac{c_r}{E_{r22}} + \frac{(1 - c_r)}{E_m}, \tag{37}$$

$$\frac{\eta_3}{G_{12}} = \frac{c_r}{G_{r12}} + \frac{(1 - c_r)}{G_m}, \tag{37}$$

where E_{r11}, E_{r22} and G_{r11} indicate the Young's moduli and shear modulus of SWCNTs, respectively, and E_m, G_m represent the corresponding properties of the isotropic matrix. The scale-dependent material properties, η_j (j= 1, 2, 3), can be calculated by matching the effective properties of structure obtained from the MD simulations with those from the rule of mixture. c_r and V_m are the volume fractions of the CNTs and matrix, respectively, which the sum of them equals to unity.

4. DQM

There is a lot of numerical method to solve the initial-and/or boundary value problems which occur in engineering domain. Some of the common numerical methods are finite element method (FEM), Galerkin method, finite difference method (FDM), DQM and etc. FEM and FDM for higher-order modes require to a great number of grid points. Therefore these solution methods for all these points need to more CPU time, while the DQM has several benefits that are listed as below (Kolahchi and Moniribidgoli 2016)

DQM is a powerful method which can be used to solve numerical problems in the analysis of structural and dynamical systems.

1. The accuracy and convergence of the DQM is higher than FEM.

2. DQM is an accurate method for solution of nonlinear differential equations in approximation of the derivatives.

3. This method can easily and exactly satisfy a variety of boundary conditions and require much less formulation and programming effort.

4. Recently, DQM has been extended to handle irregular shaped.

Due to the above striking merits of the DQM, in recent years the method has become increasingly popular in the numerical solution of problems in engineering and physical science. The main idea of the DQM is that the derivative of a function at a sample point can be approximated as a weighted linear summation of the function value at all of the sample points in the domain. The functions $f=\{u,\ w,\ \psi\ \}$ and their k^{th} derivatives with respect to x can be approximated as (Ghorbanpour Arani *et al*. 2015)

$$\frac{d^n f(x_i)}{dx^n} = \sum_{j=1}^{N} C_{ij}^{(n)} f(x_j) \qquad n = 1,...,N-1, \tag{38}$$

where N is the total number of nodes distributed along the x-axis and C_{ij} is the weighting coefficients, the recursive formula for which can be found in (Ghorbanpour Arani *et al*. 2013, 2015b). The cosine pattern is used to generate the DQ point system

$$X_i = \frac{L}{2}\left[1-\cos\left(\frac{i-1}{N_x-1}\right)\pi\right] \qquad i = 1,...,N. \tag{39}$$

Using DQM, the governing equations can be expressed in matrix form as

$$\left(\underbrace{\begin{bmatrix} [K_{bb}]_{n\times n} & [K_{bd}]_{n\times(NN-n)} \\ [K_{db}]_{(NN-n)\times n} & [K_{dd}]_{(NN-n)\times(NN-n)} \end{bmatrix}}_{[K_L+K_{NL}]} + P\underbrace{\begin{bmatrix} [Kg_{bb}]_{n\times n} & [Kg_{bd}]_{n\times(NN-n)} \\ [Kg_{db}]_{(NN-n)\times n} & [Kg_{dd}]_{(NN-n)\times(NN-n)} \end{bmatrix}}_{[K_g]}\right)_{NN\times NN} \begin{Bmatrix} \{d_b\}_{n\times 1} \\ \{d_d\}_{(NN-n)\times 1} \end{Bmatrix} = 0\ , \tag{40}$$

where K_L is the linear stiffness matrix; K_{NL} is the nonlinear stiffness matrix and K_g is geometric stiffness matrix. Also, d_b and d_d represent boundary and domain points. Noted that n and NN are 6 and 2N for Euler and 8 and 3N for Timoshenko beam model. Finally, based on an iterative method and eigenvalue problem, the buckling load of structure may be obtained.

5. Numerical results

In this section, a concrete column with elastic modules of $E_m=20\ GPa$ is considered which is reinforced with SWCNTs with elastic modules of $E_r=1\ TPa$. Based on DQM, the buckling load of structure is calculated and the effects of SWCNT volume percent, geometrical parameters, elastic foundation and boundary conditions are showed.

5.1 Accuracy of DQM

The effect of the grid point number in DQM on the buckling load of the concrete column is

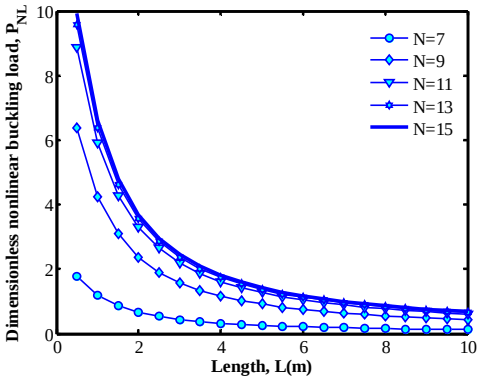

Fig. 2 Accuracy of DQM for Euler-Bernoulli beam model

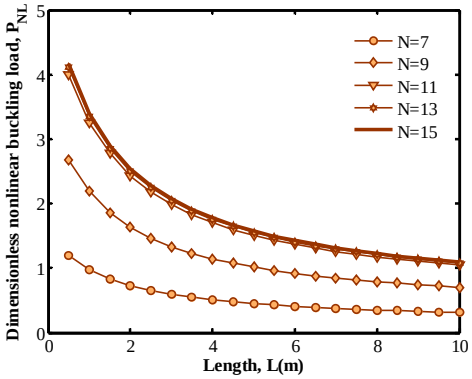

Fig. 3 Accuracy of DQM for Timoshenko beam model

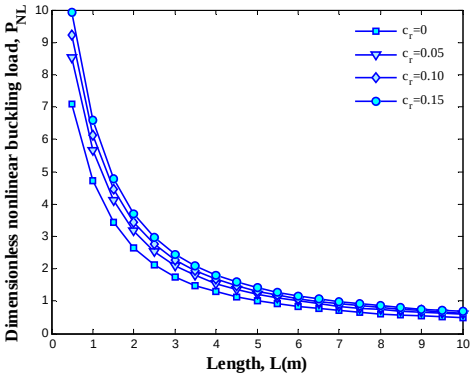

Fig. 4 The effect of SWCNT volume percent on buckling load for Euler-Bernoulli beam model

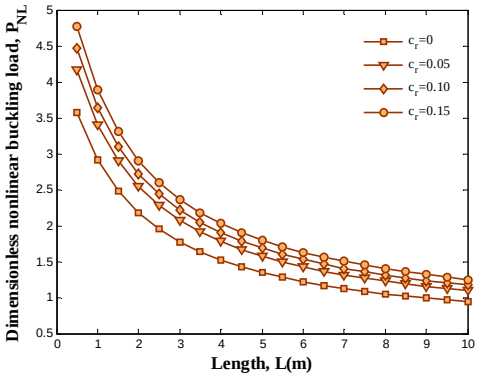

Fig. 5 The effect of SWCNT volume percent on buckling load for Timoshenko beam model

demonstrated in Figs. 2 and 3 for Euler-Bernoulli and Timoshenko beam models, respectively. As can be seen, fast rate of convergence of the method are quite evident and it is found that 15 DQM grid points can yield accurate results. In addition, with increasing length of column, the buckling load decreases due to reduction in stiffness of system.

5.2 The effect of different parameters

The effect of volume percent of SWCNTs on the nonlinear buckling load of concrete column is illustrated in Figs. 4 and 5 for Euler-Bernoulli and Timoshenko beam models, respectively. It can be found that with increasing the volume percent of SWCNTs, the nonlinear buckling load increases. It is due to the fact that with increasing volume percent of SWCNTs, the stiffness of structure increases. Hence, the SWCNT volume fraction is effective controlling parameters for buckling of the concrete column. In addition, the buckling load predicted by Euler-Bernoulli model is higher that Timoshenko one. It is because that the flexibility of Timoshenko model is higher that Euler-Bernoulli model. Hence, the results predicted by Timoshenko beam model is more real with respect to Euler-Bernoulli one.

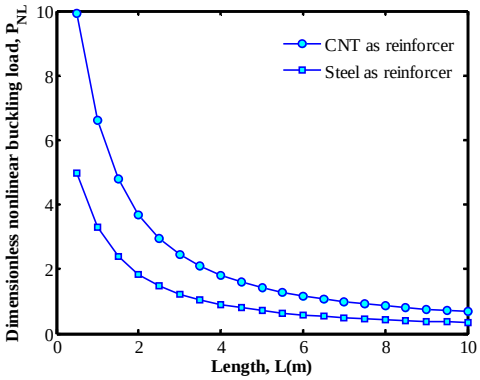

Fig. 6 Comparison of steel and SWCNT as reinforcer for Euler-Bernoulli beam model

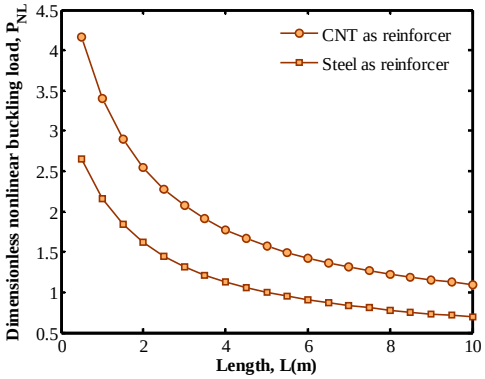

Fig. 7 Comparison of steel and SWCNT as reinforcer for Timoshenko beam model

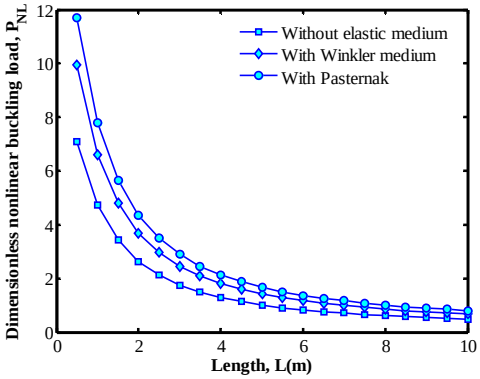

Fig. 8 The foundation effect on buckling load for Euler-Bernoulli beam model

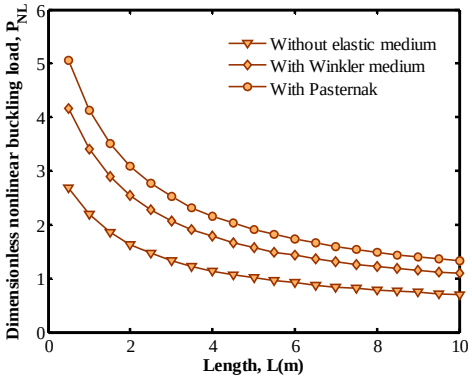

Fig. 9 The foundation effect on buckling load for Timoshenko beam model

Comparison of buckling load of concrete column reinforced with steel and SWCNTs is depicted in Figs. 6 and 7, respectively for Euler-Bernoulli and Timoshenko beam models. As can be seen, for both models, the buckling load of concrete column reinforced with SWCNT is higher with respect to concrete column reinforced with steel. However, it can be concluded that the use of nanotechnology in concrete column may improve the buckling behaviour of system. Hence, using from SWCNTs as reinforcer can be suggested in concrete structure in further.

Figs. 8 and 9 illustrate the influence of elastic medium on the buckling load along the length respectively for Euler-Bernoulli and Timoshenko beam models. Obviously, the foundation has a significant effect on buckling of the column, since the buckling load of the system in the case of without foundation are lower than other cases. It can be concluded that the buckling load for Pasternak model (spring and shear constants) is higher than Winkler (spring constant) one. The above results are reasonable, since the Pasternak medium considers not only the normal stresses (i.e. Winkler foundation) but also the transverse shear deformation and continuity among the spring elements.

The effect of boundary condition on the buckling load of structure is showmen in Figs. 10 and 11 for Euler-Bernoulli and Timoshenko beam models, respectively. It can be found that the

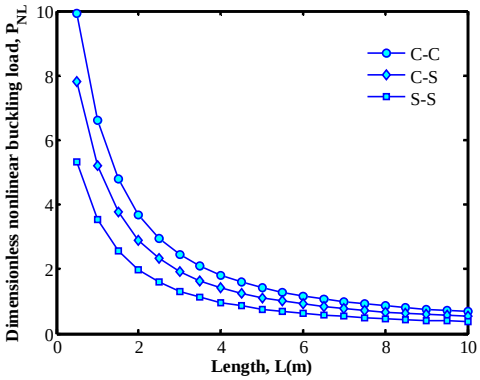

Fig. 10 The boundary condition effect on buckling load for Euler-Bernoulli beam model

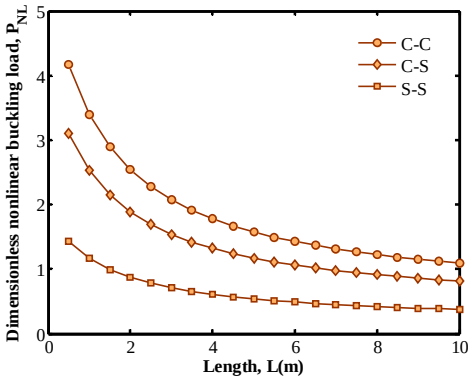

Fig. 11 The boundary condition effect on buckling load for Timoshenko beam model

maximum buckling load is related to C-C boundary condition. It is reasonable since the stiffness of C-C structure is higher.

6. Conclusion

The paper presents a new model for the concrete column armed with SWCNT theoretically for the first time. The Euler-Bernoulli and Timoshenko beam models were used for mathematical modelling and the characteristics of the equivalent composite being determined using Mixture low. DQM and a direct iterative approach were employed to obtain the nonlinear buckling load for different boundary conditions. Results indicate that with increasing the volume percent of SWCNTs, the nonlinear buckling load increases. In addition, the buckling load predicted by Euler-Bernoulli model was higher that Timoshenko one. It was also worth to mention that the buckling load of concrete column reinforced with SWCNT is higher with respect to concrete column reinforced with steel. Obviously, the foundation has a significant effect on buckling of the column, since the buckling load of the system in the case of without foundation were lower than other cases. Furthermore, the maximum buckling load was related to C-C boundary condition. In conclusion, the nanotechnology has an important role in improving the buckling of concrete column.

References

Bae, S., Mieses, A.M. and Bayrak, O. (2005), "Inelastic buckling of reinforcing bars", *J. Struct. Eng.*, **131**(2), 314-321.

Bajc, U., Saje, M., Planinc, I. and Bratina, S. (2015), "Semi-analytical buckling analysis of reinforced concrete columns exposed to fire", *Fire Safety J.*, **71**, 110-122.

Brush, D.O. and Almroth, B.O. (1975), *Buckling of bars, plates and shells*, McGraw-Hill, New York.

Dhakal, R.P. and Maekawa, K. (2002a), "Modeling for postyield buckling of reinforcement", *J. Struct. Eng.*, **128**(9), 1139-1147.

Dhakal, R.P. and Maekawa, K. (2002b), "Reinforcement stability and fracture of cover concrete in reinforced concrete members", *J. Struct. Eng.*, **128**(10), 1253-1262.

El-Helou, R.G. and Aboutaha, R.S. (2015), "Analysis of rectangular hybrid steel-GFRP reinforced concrete beam columns", *Comput. Concrete*, **16**(10), 245-260.

Engesser, F. (1889), "Über die knickfestigkeit gerader stäbe", *Z. Archit. Ing. Ver. Hann.*, **35**, 455-462.

Ghorbanpour Arani, A., Abdollahian, M. and Kolahchi, R. (2015), "Nonlinear vibration of embedded smart composite microtube conveying fluid based on modified couple stress theory", *Polym. Composite.*, **36**(7), 1314-1324.

Ghorbanpour Arani, A., Kolahchi, R. and Maraghi, Z.K. (2013), "Nonlinear vibration and instability of embedded double-walled boron nitride nanotubes based on nonlocal cylindrical shell theory", *Appl. Math. Model.*, **37**(14), 7685-7707.

Ghorbanpour Arani, A., Kolahchi, R. and Zarei, M.S. (2015), "Visco-surface-nonlocal piezoelasticity effects on nonlinear dynamic stability of graphene sheets integrated with ZnO sensors and actuators using refined zigzag theory", *Compos. Struct.*, **132**, 506-526.

Hwang, J.H., Lee, D.H., Park, M.K., Choi, S.H., Kim, K.S. and Pan, Z. (2015), "Shear performance assessment of steel fiber reinforcedprestressed concrete members", *Comput. Concrete*, **16**(9), 825-846.

Kolahchi, R. and Moniribidgoli, A.M. (2016), "Size-dependent sinusoidal beam model for dynamic instability of single-walled carbon nanotubes", *Appl. Math. Mech.*, **37**(2), 265-274.

Kolahchi, R., Bidgoli, A.M.M. and Heydari, M.M. (2015b), "Size-dependent bending analysis of FGM nano-sinusoidal plates resting on orthotropic elastic medium", *Struct. Eng. Mech.*, **55**(5), 1001-1014.

Kolahchi, R., Bidgoli, M.R., Beygipoor, G. and Fakhar, M.H. (2015a), "A nonlocal nonlinear analysis for buckling in embedded FG-SWCNT-reinforced microplates subjected to magnetic field", *J. Mech. Sci. Tech.*, **29**(9), 3669-3677.

Krauberger, N., Saje, M., Planinc, I. and Bratina, S. (2007), "Exact buckling load of a restrained RC column", *Struct. Eng. Mech.*, **27**(3), 293-310.

Lopes, A.V., Lou, T. and Lopes, S.M. (2015), "Numerical modelling of nonlinear behaviour of prestressed concrete continuous beams", *Comput. Concrete*, **15**(3), 391.

Mau, S.T. (1990), "Effect of tie spacing oninelastic buckling of reinforcing bars", *ACI Struct. J.*, **87**(6), 617-677.

Mau, S.T. and El-Mabsout, M. (1989), "Inelastic buckling of reinforcing bars", *J. Eng. Mech.*, **115**(1), 1-17.

Pantazopoulou, S.J. (1998), "Detailing for reinforcement stability in RC members", *J. Struct. Eng.*, **124**(6), 623-632.

Shanley, F.R. (1947), "Inelastic column theory", *J. Aeronaut. Sci.*, **14**, 261-264.

Vijai, K., Kumutha, R. and Vishnuram, B.G. (2015), "Flexural behaviour of fibre reinforced geopolymer concrete composite beams", *Comput. Concrete*, **15**(3), 437-459.

CC